

# Electrochemical Synthesis of Silver Nanoparticles under Protection of Poly(*N*-vinylpyrrolidone)

Bingsheng Yin,<sup>†,‡</sup> Houyi Ma,<sup>\*,†,‡</sup> Shuyun Wang,<sup>§</sup> and Shenhao Chen<sup>†,⊥</sup>

Key Laboratory for Colloid and Interface Chemistry of State Education Ministry, Shandong University, Jinan 250100, China; Department of Chemistry, Shandong University, Jinan 250100, China; Testing Center, Shandong Teachers' University, Jinan 250014, China; and State Key Laboratory for Corrosion and Protection of Metals, Shenyang 110015, China

Received: April 7, 2003; In Final Form: June 14, 2003

A novel electrochemical method for size-controlled synthesis of spherical silver nanoparticles in aqueous phase was developed for the first time. In this method the poly(*N*-vinylpyrrolidone) (PVP) was used as the stabilizer for the silver clusters. PVP was found to greatly promote silver particle formation rate and significantly reduce silver deposition rate, thereby making monodispersed silver nanoparticles to be synthesized very convenient by means of electroreduction of the bulk silver ions. It is possible to control the particle size by adjusting electrolysis parameters and to improve homogeneity of silver particles by changing the composition of electrolytic solutions. The results also showed the fact that the rate of transfer of PVP-stabilized silver clusters from the cathodic vicinity to the bulk solution played an important role in preparation of the monodispersed nanoparticles. In addition, the silver nanoparticles synthesized electrochemically may be directly employed to prepare the silver-doping tin electrodeposited coating.

## 1. Introduction

The synthesis of nanosized noble metal particles has attracted considerable interest in various fields of chemistry due to their novel physicochemical properties differing significantly from macroscopic metal phases and their potential applications in many areas, such as optics, microelectronics, catalysis, mechanics, information storage, and energy conversion.<sup>1–9</sup> The shape and size of nanoparticles greatly affect properties of metals on the nanometer scale,<sup>10</sup> and it is therefore critical to develop an effective method for preparation of nanoparticles with well-controlled shape and size. Small metal particles are usually prepared by chemical reduction of metal salts and sometimes can be processed into monodispersed nanoparticles with controllable composition and structure in large quantities.<sup>1,2,11,12</sup> Generally, the actual size of the nanoparticles obtained varies from system to system, not only because the stabilizer, the reducing agent, and the nature of the metal are varied but also because other parameters such as solvent, concentration, temperature, and reaction time are different. To make things worse, in some publications experimental details concerning these parameters are not provided,<sup>13</sup> as Bradley says that true control of particle size remains the most attractive goal for the synthetic chemists in this field.<sup>14</sup>

Electrochemistry has not been employed as a means of preparing large numbers of metal nanoparticles,<sup>15</sup> but some advantages of electrochemical methods over chemical ones in synthesis of small metal particles are the high purity of the particles and the possibility of a precise particle size control achieved by adjusting current density or applied potential.<sup>16</sup>

Reetz' and co-workers' results indicated for the first time that size-selective nanosized transition metal particles could be prepared electrochemically by using tetraalkylammonium salts as stabilizers for the metal clusters in nonaqueous medium.<sup>13,17</sup> Very recently, pulsed sonoelectrochemical synthesis, which was first introduced by Reisse et al.<sup>18</sup> and involves alternating sonic and electric pulses, has been employed to obtain shape-controlled synthesis of nanostructured materials.<sup>19</sup> Well-defined nanowires and nanorods of metals or compounds have been prepared by means of electrodeposition in membrane templates<sup>20</sup> or at step edges on graphite.<sup>21</sup> Gold nanorods have also been synthesized via this electrochemical method by introducing a shape-inducing cosurfactant.<sup>22</sup> Wiley et al.<sup>23</sup> and Bartlett et al.<sup>24</sup> have reported other forms of electrochemical metal deposition. However, in aqueous medium noble metal ions can be coated on the cathode more easily, so there exist some difficulties when noble nanoparticles are produced by the electrochemical method in this phase. In this study we report for the first time an easier and more convenient electrochemical method to prepare large numbers of well-dispersed silver nanoparticles in aqueous phase under the protection of poly(*N*-vinylpyrrolidone) (PVP) and demonstrate that the particle size distribution may be further improved by adding anionic surfactants of appropriate concentration to the electrolyte. The role of PVP is found to accelerate the silver particle formation and lower the silver deposition on cathode. Consequently, an external excitation system such as ultrasonication is no longer required, which significantly simplifies the synthesis procedure. This electrochemical method will make possible large-scale preparation of the size-controlled metal nanoparticles, especially noble metals, such as gold, platinum, and silver.

In addition, the nanoparticles protected by PVP may be directly applied in the electroplating system. The preliminary results show that silver particle can improve the tin coating in

<sup>†</sup> Key Laboratory for Colloid and Interface Chemistry of State Education Ministry, Shandong University.

<sup>‡</sup> Department of Chemistry, Shandong University.

<sup>§</sup> Shandong Teachers' University.

<sup>⊥</sup> State Key Laboratory for Corrosion and Protection of Metals.

\* Corresponding author: Fax +86-531-8565167; e-mail hyma@sdu.edu.cn.

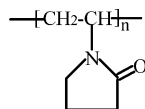


**Figure 1.** Structural scheme of the PVP molecule. Here  $n$  represents the polymerization number.  $n = 360$  for PVPK30.

the shape and size of crystallite grains on the electrochemically generated plating surface.

## 2. Experimental Section

**2.1. Synthesis of Silver Nanoparticles.** The synthesis of silver nanoparticles was performed in a simple two-electrode cell by using an EG&G M173 potentiostat/galvanostat. Seeing that the difference in radius and lattice parameters for platinum and silver is advantageous to particle formation,<sup>16</sup> a 0.5 cm  $\times$  2.0 cm platinum sheet was used here as cathode and a 20 cm long coiled platinum wire as anode, the two being 5 cm apart.

All chemicals were of analytical grade and were used without further purification. The electrolytic solutions consisted of  $\text{KNO}_3$  (0.1 mol  $\text{dm}^{-3}$ ),  $\text{AgNO}_3$  ( $5.0 \times 10^{-3}$  mol  $\text{dm}^{-3}$ ), and poly(*N*-vinylpyrrolidone) (PVP) (BASF). Figure 1 shows the structural scheme of a PVP molecule. PVPK30, whose average molecular weight ( $\bar{M}_w$ ) is about 40 000<sup>25</sup> (polymerization degree ( $n$ )  $\approx$  360<sup>26</sup>), served as the main stabilizer for silver nanoparticles synthesized in most experiments involving PVP. Two kinds of other PVP reagents which are only different from PVPK30 in the alkyl chain length, PVPK17 ( $\bar{M}_w$  10 000) and PVPK90 ( $\bar{M}_w$  360 000), were used to investigate the dependence of PVP chain length on the size of silver particles electrochemically synthesized. The PVP reagent used in the experiments was K30 unless otherwise stated. The electrolysis was carried out in the potentiostatic manner at room temperature ( $\sim 22^\circ\text{C}$ ) under mechanical stirring (or ultrasonication). The current density chosen was given by adjusting the applied potential.

**2.2. Characterization of Silver Nanoparticles.** The shape and size were measured by a transmission electron microscope (TEM) Hitachi H-800 operated at 200 kV accelerating voltage. Samples were prepared by adding ethanol to a fraction of the silver colloid synthesized, and droplet of it was dropped on a carbon-coated copper grid. The optical behavior of silver colloid was studied by a HP8453 UV-vis spectrophotometer. The interaction between silver particles and PVP was investigated by using the Nicolet Magna 750 FTIR spectrophotometer.

**2.3. Voltammetric Characterization.** A 2.0 mm diameter platinum rod (99.9%) was embedded in epoxy resin mold, and only its cross section was allowed to contact the electrolytic solution.

The cyclic voltammetric measurements were carried out in a conventional three-electrode cell at the room temperature by using a Zahner IM6 electrochemical workstation. The platinum rod electrode was used as the working electrode; a 2.0 cm  $\times$  2.0 cm platinum sheet and a saturated calomel electrode (SCE) were used as the auxiliary electrode and the reference electrode, respectively. The reference electrode was led to the surface of the working electrode through a salt bridge full of 0.2 mol  $\text{dm}^{-3}$   $\text{KNO}_3$  solution to avoid the reaction between chloride ions in SCE and silver ions in the electrolyte.

Cyclic voltammograms (CVs) for the platinum rod electrode in 0.1 mol  $\text{dm}^{-3}$   $\text{KNO}_3$  +  $5.0 \times 10^{-3}$  mol  $\text{dm}^{-3}$   $\text{AgNO}_3$  mixed solutions with and without PVP were obtained through linear potential scan from the open-circuit potential ( $E_{oc}$ ) to the designated negative vertex potential (0 V vs. SCE), then to the given positive vertex potential (1.0 V vs. SCE), and finally backward to the initial potential at a scan rate of 20  $\text{mV s}^{-1}$ . Before each CV measurement, the platinum rod was pretreated

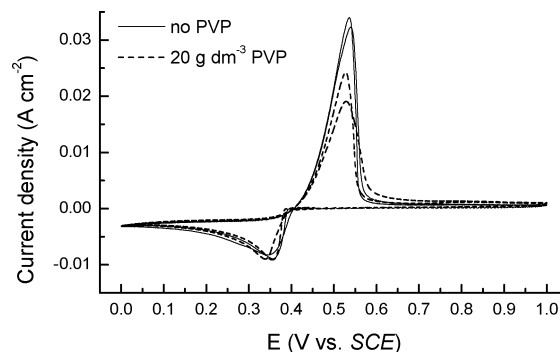


**Figure 2.** Cyclic voltammograms for the platinum rod electrode in 0.1 mol  $\text{dm}^{-3}$   $\text{KNO}_3$  +  $5.0 \times 10^{-3}$  mol  $\text{dm}^{-3}$   $\text{AgNO}_3$  mixed solutions with and without PVPK30.

in the following two steps so that a fresh and clean platinum surface could be obtained: (I) The rod was first immersed in 1:1  $\text{HNO}_3$  solution (volume ratio between concentrated  $\text{HNO}_3$  and  $\text{H}_2\text{O}$ ) for 5 min to remove reductive substances on its surface, and (II) it was afterward galvanostatically reduced in a deoxygenated 0.2 mol  $\text{dm}^{-3}$   $\text{KNO}_3$  solution at a cathodic current density of 1  $\text{mA cm}^{-2}$  for 5 min in order to reduce the oxidizing substance on the electrode surface.

**2.4. Application of Silver Nanoparticles in Tin Electroplating.** A bath solution used in the study was 1.0 mol  $\text{dm}^{-3}$   $\text{H}_2\text{SO}_4$  + 0.15 mol  $\text{dm}^{-3}$   $\text{SnSO}_4$  mixed solution, containing 4 g  $\text{dm}^{-3}$  nonionic dampening agent.

Electroplating was done in a 250 mL two-electrode cell at room temperature ( $\sim 22^\circ\text{C}$ ) by using an EG&G M173 potentiostat/galvanostat. The anode was a 4.5 cm  $\times$  4.5 cm graphite sheet, and the cathode was a 4.5 cm  $\times$  4.5 cm copper sheet, the two being 10 cm apart. This electroplating process was carried out in a galvanostatic manner, with an applied current density (10  $\text{mA cm}^{-2}$ ). Subsequently, silver nanoparticle colloid previously synthesized was added into the bath electrolyte. In this way, silver-doping tin electrodeposited coating was prepared. To investigate the influence of the silver particle on the microstructure of the tin coating, pure tin plating was also prepared under identical experimental conditions. The surface morphology of the two coatings was observed through the scanning electron microscope (SEM).

## 3. Results and Discussion

**3.1. Role of PVP.** It was observed that silver ions were soon electrodeposited on the platinum cathode in the PVP-free electrolytic solution after the electrolysis process began, but this situation completely changed with the addition of PVP to the electrolyte. A typical experiment was performed in a PVP-containing electrolyte under static conditions. Electrolyte around the cathode gradually changed in color from a light yellow at the initial reaction to a dark yellow at the end of reaction; the yellow substance diffused slowly from the cathode surface to the bulk during electrolysis. The appearance of the yellow color reveals formation of silver nanoparticles. Interestingly, the cathode was found slightly black after the experiment was over. This phenomenon is attributed to the existence of a competition between two different cathode surface processes according to Rodriguez-Sanchez et al.<sup>16</sup> One process is the silver particle formation, and the other is the silver deposition on cathode. It is concluded that PVP greatly enhances the former and effectively reduces the latter. This conclusion is supported by cyclic voltammetric results.

Figure 2 shows the CVs of platinum rod electrode in the PVP-containing solution and the PVP-free solution. Each cyclic

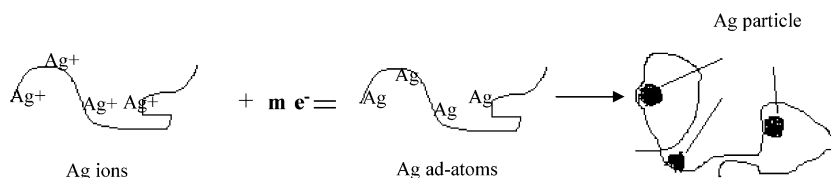


**Figure 3.** Schematic diagram showing formation of electrochemically produced PVP-stabilized silver clusters.

voltammogram exhibits one reduction peak at 0.53 V (peak A) and a large oxidation peak centered at 0.36 V (peak B) in the potential range (0–1.0 V) to be investigated, regardless of presence or absence of PVP. The reduction peak is attributed to electrodeposition of silver ions on the platinum surface, and the oxidation peak is related to oxidation of the silver electrodeposition. A comparison of the two CVs shows that there is no marked difference between the two cathodic peaks; however, the anodic current peak obtained in the absence of PVP is higher than that obtained in the presence of PVP. In the PVP-free solution, silver ions to be reduced almost completely deposited on the surface of the platinum rod electrode when the potential was swept negatively, whereas in the PVP-containing solution, the silver ions reduced were divided into two parts: one part was electrodeposited on the platinum surface, forming the silver deposition, and the other was reduced to silver nanoparticles stabilized by PVP when the potential was scanned toward negative direction. Thus, in the PVP-free solution all metallic silver produced in the negative sweep, namely the silver electrodeposition, was completely oxidized, turning into  $\text{Ag(I)}$  species, while in the PVP-containing solution only silver electrodeposition was oxidized again when the potential was positively scanned. This is the reason why CVs measured in PVP-containing solution give a small oxidation, but those measured in PVP-free solution exhibit a relatively larger oxidation peak.

The key to electrochemical synthesis of silver nanoparticles in aqueous phase is to avoid formation of silver plating and to force silver particles reduced to leave the cathode surface as rapidly as possible. In this sense, PVP may fully meet the requirements for electrochemical synthesis of silver nanoparticles. We also carried out contrast tests by using other compounds such as tetraalkylammonium salts ( $\text{R}^4\text{N}^+\text{X}^-$ ) and sodium dodecyl benzenesulfonate (SDBS) as stabilizers; however, it was seen that silver ions were soon electrodeposited on the platinum cathode rather than reduced to silver particles.

The protective mechanism of PVP in the electrochemical synthesis of silver particles is generally proposed on the basis of its structural features. PVP has a structure of a polyvinyl skeleton with polar groups, as is shown in Figure 1. The donated lone pairs of both nitrogen and oxygen atoms in the polar groups of one PVP unit may occupy two sp orbitals of silver ions to form a complex compound.<sup>26</sup>

The first step is the formation of coordinative bonding between PVP and silver ions, producing the  $\text{Ag}_m^{m+}$ –PVP complex (see Figure 3), in which  $m$  is the number of silver ions anchored at a PVP molecule. This case also occurs in the chemical reduction process of silver ions in the presence of PVP.<sup>25–27</sup>

The second step is the electrochemical reduction of the  $\text{Ag}_m^{m+}$ –PVP complex at the cathode/electrolyte interface, producing silver adatoms ( $\text{Ag}_m^0$ –PVP) protected by PVP. In this step, the influence of the chemical bond must be considered. Since the ligand of C–N and C=O in PVP contributes more electronic density to the sp orbital of silver ions than  $\text{H}_2\text{O}$  does, the silver ions in the  $\text{Ag}_m^{m+}$ –PVP complex may obtain electrons more easily from the cathode than those in the  $\text{Ag}^+$ – $\text{H}_2\text{O}$  complex. Thus, the presence of PVP ensures that the  $\text{Ag}_m^{m+}$ –

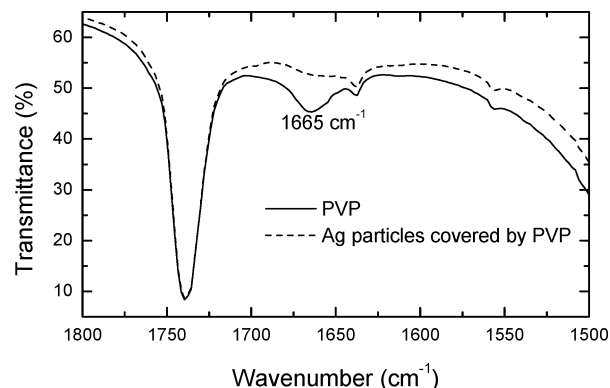


**Figure 4.** FTIR spectra for the PVP and silver nanoparticles covered by PVP in wavenumber between 1800 and 1500  $\text{cm}^{-1}$ .

PVP complex rather than single  $\text{Ag}^+$  ion is reduced. In this way, the silver deposition trend at cathode surface will be effectively lowered.

The subsequent step is PVP-accelerated formation of a large amount of silver nuclei. It was found in our experiments that the color of the solution in the vicinity of cathode changed from a light yellow to a dark yellow and then to gray, whereas a gray color always appeared during electroreduction of silver ions in the absence of PVP. On the basis of Zhang and co-workers' results,<sup>26</sup> it is inferred that the scattering of sunlight by nuclei with a diameter smaller than 10 nm is responsible for the light yellow color.

The fourth step is that coalescence of the silver clusters during the growth progress is prevented since the PVP has the role to promote silver nucleation and to prohibit grain growth and particle aggregation. The steric effect arising from long polyvinyl chain of PVP on the surface of silver particles can contribute to antiagglomeration, whereas the chemical bond between the PVP and silver powders may prohibit aggregation of silver particles. The large particles obtained through ultracentrifugation were washed in water and ethanol three times, dried in a vacuum, and were finally redispersed in ethanol. Figure 4 shows the FTIR spectra for the silver particles and pure PVP. The only difference between the two spectra is that in the spectrum for silver particles the bond at 1665  $\text{cm}^{-1}$  corresponding to the C=O stretching vibration disappears. This verifies that PVP molecules strongly adsorb on the surface of silver particles through the coordination bond between the silver atom and oxygen atom of the carbonyl group and therefore cannot be washed out.

The influence of PVPK30 concentration on the silver particle size was studied through UV–vis spectroscopy. Figure 5 shows a group of UV–vis absorption spectra for the electrolytic solutions with different PVP monomer/ $\text{Ag}^+$  molar ratios obtained at the same electrolysis time. In the case of relatively low molar ratio ( $\leq 10:1$ ), no obvious absorbance band is observed, as is shown by curves A–C in Figure 1. In addition, the electrolytes after 3 min electrolysis seemed to be grayish, which implies formation of large silver particles due to insufficient protection of PVP. Usually, the steric effect of PVP is determined to a great extent by the coverage of PVP on the



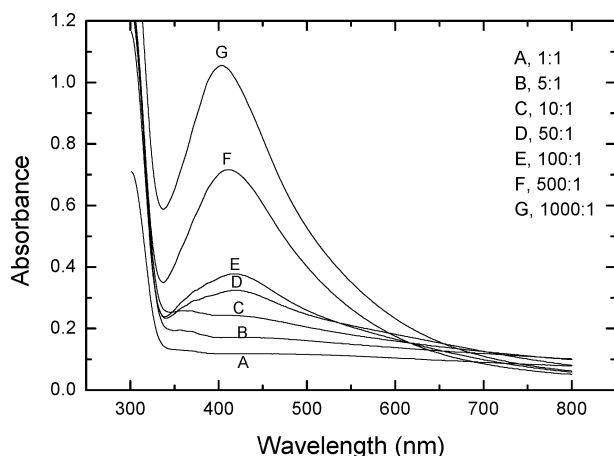


**Figure 5.** UV-vis spectra for silver nanoparticles synthesized by electrochemical reduction in electrolytes with different PVP monomer/ $\text{Ag}^+$  molar ratios under mechanical stirring (electrolysis time is 180 s). PVP/ $\text{Ag}^+$  molar ratios are indicated in the plot.

surface of silver particles; it is therefore necessary to provide appropriately high PVP concentration for PVP adsorption on silver particles. A lower PVP monomer/ $\text{Ag}^+$  molar ratio may be insufficient to provide steric stabilization, probably resulting in particle aggregation.<sup>25,26</sup> The PVP protection effect obviously improves with the increasing ratio, as is expected. When the ratio increases to 50:1, a broad absorption band centered at 420 nm, which is the characteristic plasmon band for silver nanoparticles, shows up. Moreover, upon increasing the ratio from 50:1 to 1000:1, the band becomes more symmetrical, and a blue shift in the maximum of plasmon peak appears. These features are associated with the small size and uniform size distribution for silver nanoparticles synthesized. However, the higher PVP monomer/ $\text{Ag}^+$  molar ratio is disadvantageous to electrochemical synthesis of ultrafine silver particles. In such a case, high PVP concentration makes the electrolyte more viscous and therefore more difficult to handle in the electrochemical synthesis process. The increase in viscosity of the electrolyte also lowers the transfer rate of silver ions toward the cathode, which increases the time necessary to complete electroreduction of silver ions. Particularly, some crimson substances appeared around the cathode soon after the electrolysis began although the bulk solution was deep yellow in color. The appropriate molar ratio between PVP monomer and silver ion ranges from 50:1 to 1000:1 based on our results.

The effect of PVP chain length on the particle size was also investigated by using UV-vis spectroscopic study. Here three PVP polymers (PVPK17, PVPK30, and PVPK90) with the same structure but different chain lengths were used as the stabilizers for silver nanoparticles. The UV-vis absorption spectra obtained with PVPK30 and PVPK90 all exhibit a well-defined broad absorbance peak, especially in the case of higher PVP concentration, whereas that obtained by using PVPK17 does not show any peak (see Figure 6) under identical conditions. Thus, we believe that PVP with a short polyvinyl chain is unfavorable for the electrochemical synthesis of monodispersed silver nanoparticles. We also noticed a fact that the silver colloids synthesized electrochemically under protection of PVPK30 and PVPK90 displayed a light yellow color and a slightly deep yellow color, respectively, which is characteristic of the color of small silver particles, but silver colloids obtained under protection of PVPK17 appeared grayish in color, indicating the formation of large silver particles,<sup>26</sup> which is caused by insufficient protection of PVPK17.

**3.2. Effect of the Stirring Method.** It should be emphasized that the silver clusters formed must be rapidly transferred from

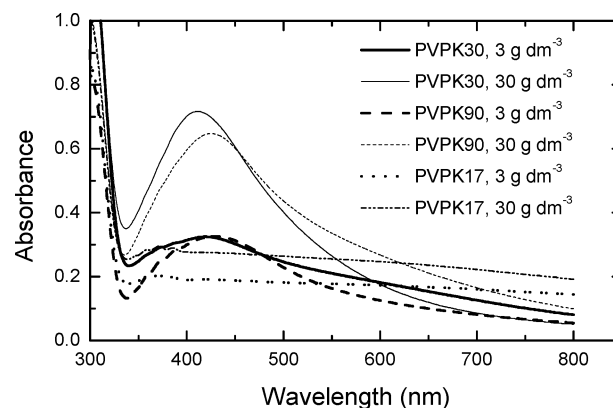


**Figure 6.** UV-vis spectra for the silver nanoparticles electrochemically synthesized at the same electrolysis time (180 s) under protection of PVP with different polyvinyl chain lengths.

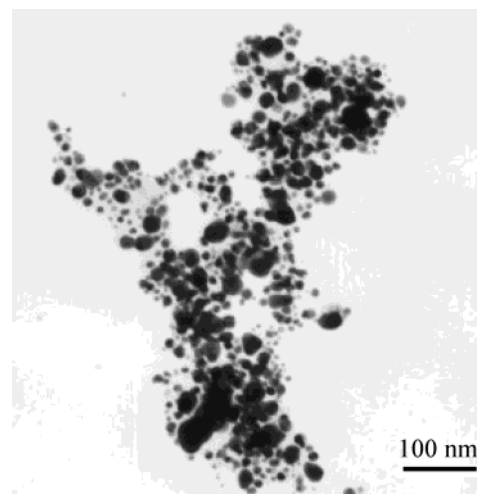
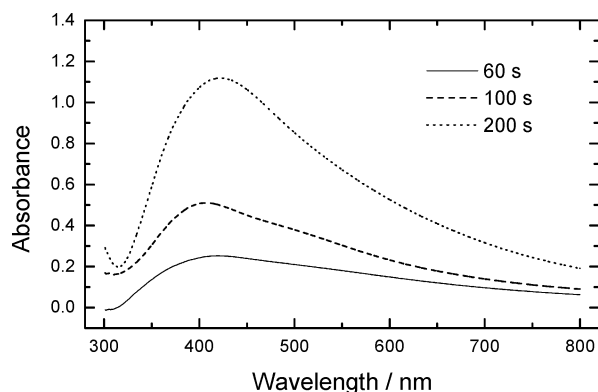


**Figure 7.** TEM image of silver nanoparticles synthesized under ultrasonic agitation.

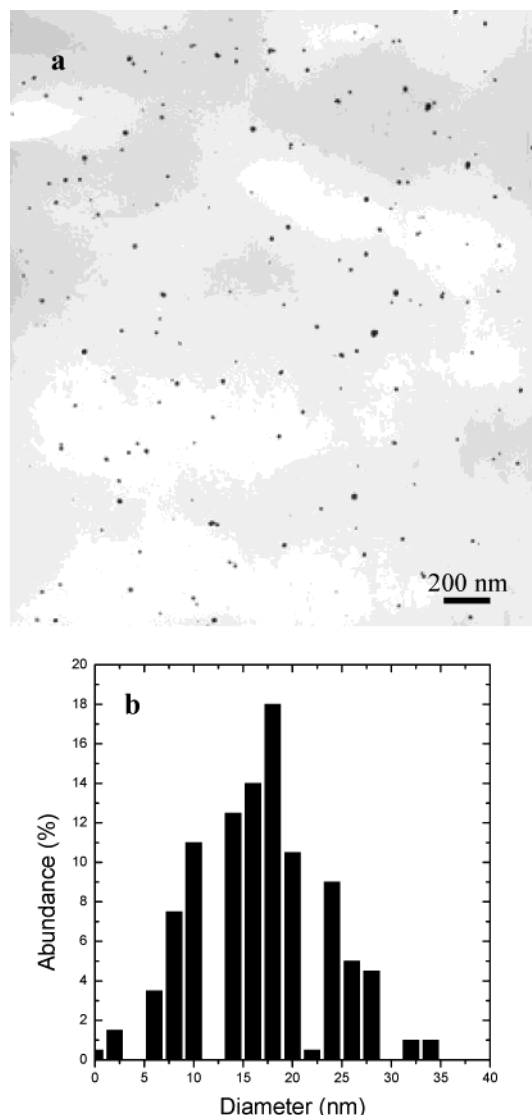
the cathodic vicinity to the bulk solution in order to obtain the nearly monodispersed nanoparticles. Otherwise, when the concentration of silver nanoparticles in the vicinity of the cathode is too high, the increase of interaction between alkyl chains of PVP will lead to the appearance of flocculates. Ultrasonication and mechanical stirring were attempted to accelerate the transfer of silver clusters to the bulk solution.

Figure 7 shows the TEM image of silver nanoparticles prepared under ultrasonication. It can be seen that the particles were spherically and multiply dispersed, and aggregation of particles occurred. Clearly, ultrasonic vibration cannot transfer the silver clusters formed from the cathodic vicinity to the bulk. Its role is just to increase the collision frequency between the silver clusters formed and the cathode. Formation of large particles can be explained on the basis of the theory of suspended electrode.<sup>19b</sup> Excited by the ultrasonic waves, the suspended silver particles move in solution near the cathode, come into collision with the cathode, accept its potential, and then travel back to the solution. These charged particles behave as part of the cathode and can make silver ions electrodeposit on them and therefore grow into large particles.

When mechanical stirring was used instead of ultrasonication, the electrolytic solution showed a beautiful variation in visible color, from light yellow to deep yellow and finally to brownish red, depending on electrolysis time, and no black precipitate took place until the end of electrolysis reaction. The color change is associated with the increase of the concentration of silver nanoparticles in the electrolyte, which is supported by the



**Figure 8.** UV-vis spectra for the silver colloidal solutions obtained in the case of different electrolysis time under mechanical stirring conditions by using PVPK32 as the stabilizer.



**Figure 9.** TEM image (a) and particle size distribution (b) of silver nanoparticles electrochemically synthesized in the presence of PVP under mechanical stirring.

evolution of the absorbance intensity at about 420 nm with the electrolysis time shown in Figure 8. The peak centered at 420 nm is the characteristic peak for silver nanoparticles.

Figure 9a gives a typical TEM photograph of silver particles prepared under mechanical stirring. The particle size distribution is shown as a histogram in Figure 9b. The Gaussian fit shows

that the mean diameter of particles is 16.6 nm and the standard deviation (SD) fitted is 6.22. It is obvious that the nanoparticles in Figure 9a are smaller in size and much better in size distribution than those shown in Figure 7. Compared to the ultrasonic agitation, the mechanical stirring can significantly accelerate the transfer of silver clusters produced from the cathodic vicinity to the bulk solution and make the silver clusters distribute relatively uniform in the solution. Thus, most silver clusters far from the cathode grow uniformly in the bulk under protection of PVP, which is favorable for formation of the well-dispersed nanoparticles. Despite all this, mechanical stirring cannot completely eliminate the formation of suspended electrode. A small amount of silver clusters near the cathode still has enough chances to grow into large particles according to the mechanism of suspended electrode formation, as stated earlier.

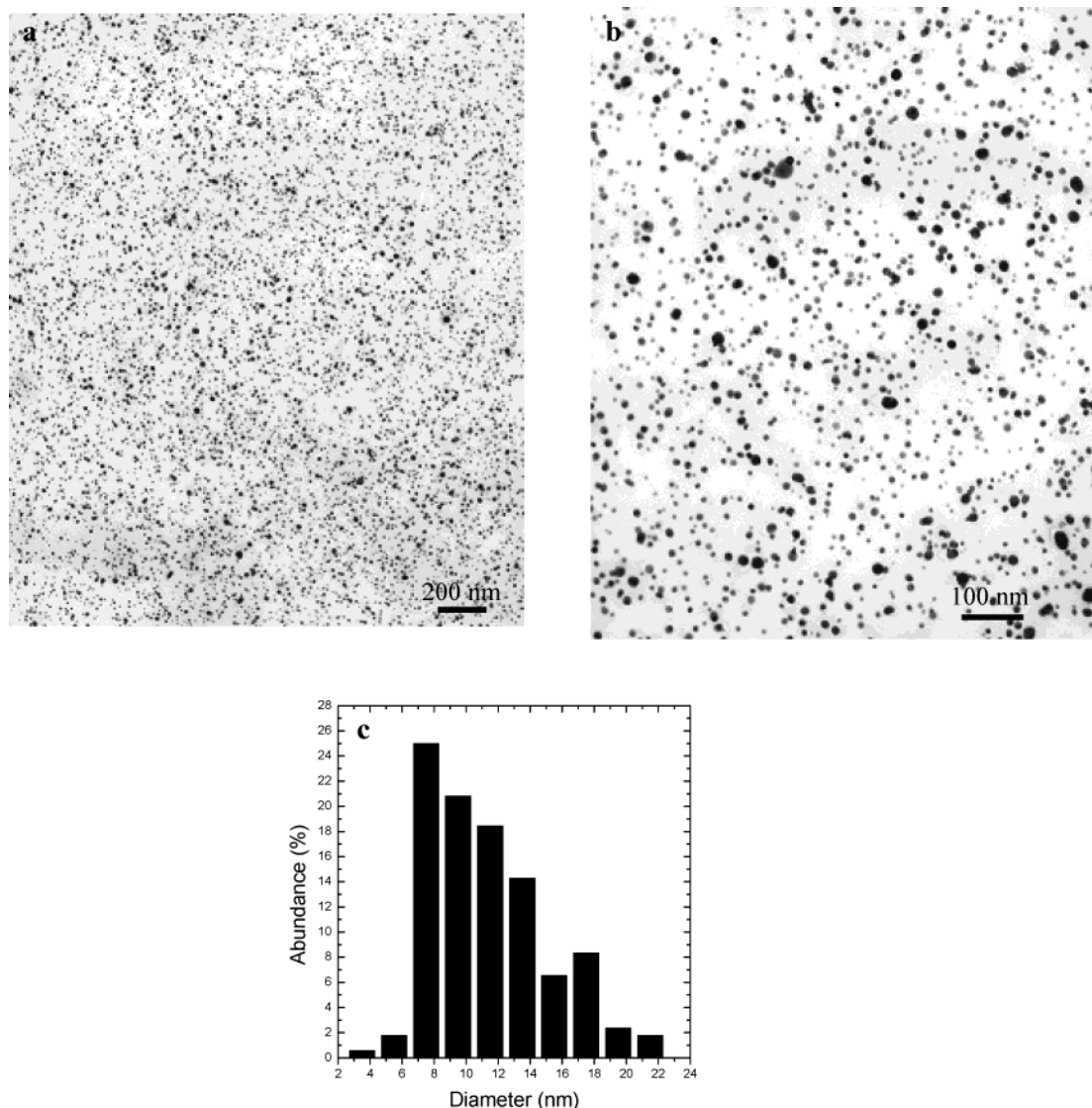
**3.3. Use of Sodium Dodecyl Benzenesulfonate (SDBS) as Costabilizer.** Provided that sodium dodecyl benzenesulfonate (SDBS) was used as costabilizer for silver clusters in the presence of PVP, under combined action of the polymer and the surfactant,<sup>28</sup> the silver particle size was further reduced and particle size distribution greatly improved. Figure 10a,b shows that the particles are nearly monodispersed, and Figure 10c indicates that most particles are in the range 7.0–14.0 nm. It was calculated through the Gaussian fit that the mean particle diameter was 10.2 nm and SD fitted was 3.43.

Figure 11 shows a set of UV-vis absorption spectra for silver nanoparticles synthesized in  $\text{KNO}_3 + \text{AgNO}_3 + \text{PVPK30}$  mixed solutions without SDBS and in the presence of various concentrations of SDBS. By comparing the absorption spectra obtained in the presence or absence of SDBS, it is found that intensity of the characteristic absorbance bands decreases, but its symmetry obviously improves in SDBS-containing solutions, which confirms the fact that silver particles are becoming better in monodispersity when using SDBS as costabilizer.<sup>25</sup>

How SDBS affects the particle size and the size distribution has been unclear at the present stage, but it is inferred that interaction of PVP and the dodecyl benzenesulfonate (DBS) anions probably resulting from van der Waals force between long carbon chains leads to formation of PVP/SDBS aggregates that are charged negatively. The aggregates combine with free silver ions more easily than PVP molecules do. However, the stronger bonding energy between the aggregates and silver ions slows the reduction rate of silver ions. In addition, the electrostatic repulsion between DBS anions and the cathode also makes the silver clusters leave the vicinity of cathode more quickly. The above two actions are beneficial for the acquirement of silver particles with smaller diameter and better size distribution.

As far as our knowledge goes, the method described in this paper is the easiest and most convenient electrochemical one to prepare spherical silver nanoparticles. The whole synthesis process is conducted in aqueous solution rather than in organic media, and all substances used are harmless to the environment. Different from previous studies,<sup>17,22</sup> the bulk metal is not converted from the sacrificial anode but comes directly from the electrolyte. The use of  $\text{KNO}_3$  as the main supporting effectively avoids the agglomeration of silver particles after depletion of silver existing in pulse sonoelectrochemical methods.<sup>19b</sup> Particularly, the backbone of PVP forms a hydrophobic domain, which enwraps silver particles, whereas hydrophilic groups of PVP interact with water, which makes silver particles distribute stably in aqueous solution.<sup>26</sup>

The most distinguished features of the method include simple operation, high yield, well-dispersity of particles, quite high stability of metal colloids prepared, easy control of particle size



**Figure 10.** TEM image with low magnification (a) and high magnification (b) and particle size distribution (c) for silver nanoparticles electrochemically synthesized in the presence of both PVP and SDBS under mechanical stirring.

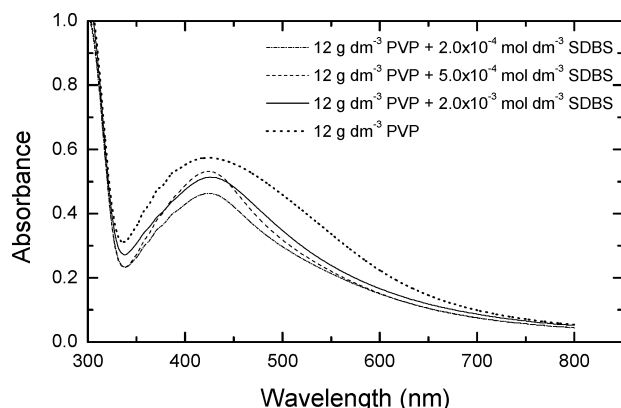


**Figure 11.** UV-vis spectra absorption for silver nanoparticles electrochemically synthesized in the KNO<sub>3</sub> + AgNO<sub>3</sub> + PVPK30 mixed electrolytes with and without SDBS under mechanical stirring.

and absence of undesired byproducts, and are especially good for future application in synthesis of metal nanoparticles on a large scale.

**3.4. Application of Silver Nanoparticles in Tin Electroplating.** The silver colloid prepared electrochemically under protection of PVP is quite stable and can be preserved several

months, without occurrence of any precipitate. Only a small amount of large particles was separated from the colloid when the silver colloid was ultracentrifuged at 8000 rpm for 10 min. Because of very high stability, the silver colloid protected by PVP can be directly used to prepare the silver-doping tin coating, which probably serves as the substitute for tin-lead composite coating harmful to the environment.

Figure 12a shows the surface morphology of the pure tin coating, and Figure 12b shows that of silver nanoparticle doping tin coating. It is seen that there existed crystallite grains with different shape, such as columned or square and irregular grains on the surface of pure tin coating; in contrast, silver nanoparticle doping tin electrodeposited coating only presented triangle grains on the surface. Clearly, the small amount of silver nanoparticle additive in the bath solution significantly changed the surface structure of tin coating. The effect of silver nanoparticles on the tin electroplating process and the other properties of tin coating are being further investigated.

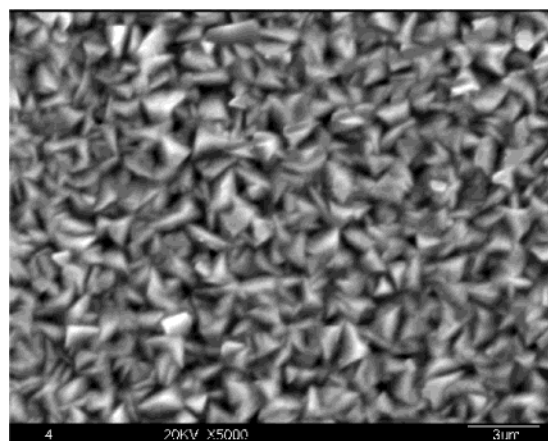
#### 4. Conclusions

In summary, a novel electrochemical method was successfully developed for the synthesis of size-controlled spherical silver nanoparticles. PVP plays a key role in the process of electrochemical synthesis of silver particles. It not only significantly





(a)



(b)

**Figure 12.** Surface microstructure of electrocoatings measured by the scanning electron microscope (SEM): (a) a pure tin coating; (b) a complex coating containing tin and silver nanoparticles.

reduces the silver deposition rate and accelerates the rate of silver particle formation at the same time but also prevents the particles formed from being agglomerated. Another necessary condition to prepare the well-dispersed particles is to accelerate the transfer of silver clusters formed from the cathodic vicinity to the bulk solution. The mechanical stirring can meet very well this kind of acquirement. In this study, the bulk metal is not converted from the sacrificial anode but comes directly from the electrolyte, which makes possible large-scale preparation of the size-controlled silver particles. The use of  $\text{KNO}_3$  as the main supporting effectively avoids the agglomeration of silver particles after depletion of silver existing in pulse sonoelectrochemical methods. The present method may be extended to synthesizing other metal nanoparticles such as gold, platinum, and copper.

**Acknowledgment.** This work was subsidized with the Scientific Research Award Fund for Excellent Middle-Aged and Young Scientists of Shandong Province (02BS053), the Youth Foundation of Shandong University and the Visiting Scholar Foundation of Key Laboratory in Shandong University, and the Special Funds for the Major State Basic Research Projects (G19990650).

## References and Notes

- (1) Sun, Y.; Xia, Y. *Science* **2002**, 298, 2176.
- (2) Jana, N. R.; Gearheart, L.; Murphy, C. J. *Chem. Commun.* **2001**, 617.
- (3) Yao, J. L.; Pan, G. P.; Xue, K. H.; Wu, D. Y.; Ren, B.; Sun, D. M.; Tang, J.; Xu, X.; Tian, Z. Q. *Pure Appl. Chem.* **2000**, 72, 221.
- (4) (a) Hu, J. T.; Odom, T. W.; Lieber, C. M. *Acc. Chem. Res.* **1999**, 32, 435. (b) McConnell, W. P.; Novak, J. P.; Brousseau, L. C.; Fuierer, R. R.; Tenent, R. C.; Feldheim, D. L. *J. Phys. Chem. B* **2000**, 104, 8925.
- (5) (a) Zhao, S.; Chen, S.; Wang, S.; Li, D.; Ma, H. *Langmuir* **2002**, 18, 3315. (b) Jana, N. R.; Wang, Z. L.; Pal, T. *Langmuir* **2000**, 16, 2457.
- (6) Ghosh, K.; Maiti, S. N. *J. Appl. Polym. Sci.* **1996**, 60, 323.
- (7) (a) Andres, P. R.; Bielefeld, J. D.; Henderson, J. I.; Janes, D. B.; Kolagunta, V. R.; Kubiak, C. P.; Mahoney, W. J.; Osifchin, R. G. *Science* **1996**, 273, 1960. (b) Andres, P. R.; Bein, T.; Dorogi, M.; Feng, S.; Henderson, J. I.; Kubiak, C. P.; Mahoney, W.; Osifchin, R. G.; Reifenberger, R. *Science* **1996**, 272, 1323.
- (8) Murray, C. B.; Sun, S.; Doyle, H.; Betley, T. *Mater. Res. Soc. Bull.* **2001**, 26, 985.
- (9) Forster, S.; Antonietti, M. *Adv. Mater.* **1998**, 10, 195.
- (10) (a) Nie, S.; Emory, S. R. *Science* **1997**, 275, 1102. (b) Buffat, P.; Borel, J.-P. *Phys. Rev. A* **1976**, 13, 3287. (c) Castro, T.; Reifenberger, R.; Choi, E.; Andres, P. R. *Phys. Rev. B* **1990**, 42, 8548. (d) Link, S.; El-Sayed, M. A. *J. Phys. Chem. B* **1999**, 103, 8410. (e) Petit, C.; Taleb, A.; Pileni, M. P. *J. Phys. Chem. B* **1999**, 103, 1805.
- (11) Schmid, G. *Chem. Rev.* **1992**, 92, 1709.
- (12) Goia, D. V.; Matijevic, E. *New J. Chem.* **1998**, 22, 1203.
- (13) Reetz, M. T.; Winter, M.; Breinbauer, R.; Thurn-Albrecht, T.; Vogel, W. *Chem.-Eur. J.* **2001**, 7, 1084.
- (14) Bradley, J. S. In *Clusters and Colloids*; Schmid, G., Ed.; VCH: Weinheim, 1994; Chapter 6.
- (15) Zoval, J. V.; Stiger, R. M.; Biernacki, P. R.; Penner, R. M. *J. Phys. Chem.* **1996**, 100, 837.
- (16) Rodriguez-Sanchez, L.; Blanco, M. C.; Lopez-Quintela, M. A. *J. Phys. Chem. B* **2000**, 104, 9683.
- (17) Reetz, M. T.; Helbig, W. *J. Am. Chem. Soc.* **1994**, 116, 7401. (b) Reetz, M. T.; Helbig, W.; Quaiser, S. A.; Stimming, U.; Breuer, N.; Vogel, R. *Science* **1995**, 267, 367.
- (18) (a) Reisse, J.; Francois, H.; Vandercammen, J.; Fabre, O.; Mesmaeker, A. K.-D.; Maerschalk, C.; Delplancke, J. L. *Electrochim. Acta* **1994**, 39, 37. (b) Delplancke, J. L.; Bella, V. D.; Reisse, J.; Winand, R. *Mater. Res. Soc. Symp.* **1995**, 372, 205. (c) Durant, A.; Delplancke, J. L.; Libert, V.; Reisse, J. *Eur. J. Org. Chem.* **1999**, 11, 2845. (d) Delplancke, J. L.; Dille, J.; Reisse, J.; Long, G. J.; Mohan, A.; Grandjean, F. *Chem. Mater.* **2000**, 12, 946.
- (19) (a) Zhu, J.; Liu, S.; Palchik, O.; Koltypin, Y.; Gedanken, A. *Langmuir* **2000**, 16, 6396. (b) Socol, Y.; Abramson, O.; Gedanken, A.; Meshorer, Y.; Berenstein, L.; Zaban, A. *Langmuir* **2002**, 18, 4736. (c) Zhu, J. J.; Aruna, S. T.; Koltypin, Y.; Gedanken, A. *Chem. Mater.* **2000**, 12, 143. (d) Mastai, Y.; Polsky, R.; Koltypin, Y.; Gedanken, A.; Hodes, G. *J. Am. Chem. Soc.* **1999**, 121, 10047.
- (20) (a) Parthasarathy, R.; Martin, C. R. *Nature (London)* **1994**, 369, 298. (b) Martin, C. R. *Adv. Mater.* **1991**, 3, 960. (c) Wu, C. G.; Bein, T. *Science* **1994**, 264, 1757. (d) Brumlik, C. J.; Martin, C. R. *J. Am. Chem. Soc.* **1991**, 113, 3174. (e) Nishizawa, M.; Menon, V. P.; Martin, C. R. *Science* **1995**, 268, 700. (f) Penner, R. M.; Martin, C. R. *Anal. Chem.* **1987**, 59, 2625. (g) Nicewarner-Pena, S. R.; Freeman, R. G.; Reiss, B. D.; He, L.; Pena, D. J.; Walton, I. D.; Cromer, R.; Keating, C. D.; Natan, M. J. *Science* **2001**, 294, 137.
- (21) (a) Zach, M. P.; Kwokh, N.; Penner, R. M. *Science* **2002**, 290, 2120. (b) Zach, M. P.; Penner, R. M. *Adv. Mater.* **2000**, 12, 878. (c) Zach, M. P.; Ng, K. H.; Penner, R. M. *Science* **2000**, 290, 2120.
- (22) (a) Mohamed, M. B.; Ismail, K. Z.; Link, S.; El-Sayed, M. A. *J. Phys. Chem. B* **1998**, 102, 9370. (b) Yu, Y.-Y.; Chang, S. S.; Lee, C.-L.; Wang, C. R. *J. Phys. Chem. B* **1997**, 101, 6661. (c) Chang, S. S.; Shih, C. W.; Chen, C. D.; Lai, W.-C.; Wang, C. R. *Langmuir* **1999**, 15, 701.
- (23) Xu, L.; Zhou, W. L.; Frommen, C.; Baughan, R. H.; Zakhidov, A. A.; Malkinski, L. M.; Wang, J.-Q.; Wiley, J. B. *Chem. Commun.* **2000**, 997.
- (24) Bartlett, P. N.; Birkin, P. R.; Ghanem, M. A. *Chem. Commun.* **2000**, 1671.
- (25) Pastoriza-Santos, I.; Liz-Marzan, L. M. *Langmuir* **2002**, 18, 2888.
- (26) Zhang, Z.; Zhao, B.; Hu, J. *Solid State Chem.* **1996**, 121, 105.
- (27) Carotenuto, G.; Peper, G. P.; Nicolais, L. *Eur. Phys. J. B* **2000**, 16, 11.
- (28) Misselyn-Bauduin, A.-M.; Thibaut, A.; Grandjean, J.; Broze, G.; Jerome, R. J. *Colloid Interface Sci.* **2001**, 238, 1.